A Simple Strategy for DRFOC of 3-phase Induction Motors under Single-phase Open Fault

Mohammad Shabandokht-Zarami[1], Mahmood Ghanbari[1,*], Esmaeil Alibeiki[1,2], Mohammad Jannati[1]

Abstract – This research investigates a simple method for Direct Rotor Field-Oriented Control (DRFOC) of star-connected 3-Phase Induction Motor (3Ph IM) drives under Single-Phase Open Fault (SPOF). The proposed control scheme includes a modified RFOC strategy in cooperation with a flux linkage observer. Most studies on this topic are intended for Indirect Rotor Field-Oriented Control (IRFOC), and hence are not appropriate at low speed operation due to using a pure integration for the flux angle calculation. To this end, a rotor flux linkage observer is designed which alleviates the speed and torque ripples of the faulty motor during low speed operation. The observer is capable of estimation of the rotor flux during healthy and SPOF conditions by only some modifications in the 3Ph IM parameters. The proposed DRFOC approach is tested under different conditions and the effectiveness of the proposed system is confirmed by experimental results. The results show the good fault tolerant capability and tracking performance of the proposed controller during different speeds.

1. Introduction

Due to the extensive merits of 3-Phase Induction Motor (3Ph IM) drives such as reduced price and size, low maintenance, and high reliability, these drives are used in different industrial applications [1-3]. In some industries e.g., electric propulsion, aerospace, and electric vehicles, the control of 3Ph IM drives during fault conditions is very crucial. For these applications, Fault-Tolerant Control (FTC) systems are appreciated. FTC systems are attracting more interests due to their ability of growing the reliability and safety of 3Ph IM drives [4-6]. In terms of the used components in a 3Ph IM drive, fault can happen in sensors (such as rotor speed sensor or stator phase current sensor), or inverter (such as power switch, DC-link), or motor (such as rotor bars or stator windings) [7].

Failure of motor phases degrades the performance of 3Ph IM drives due to high speed and torque ripples or even leads to the shutdown of the entire system. Single-Phase Open Fault (SPOF) is the most common type of failure in 3Ph IM drives. This type of fault can happen in a 3Ph IM drive because opening of the stator windings or power switch short-circuit fault [8]. The percentage of motor failures produced by this fault is up to 37% [9]. It is worth noting that FTC of 3Ph IM drives against SPOF includes three aspects: fault diagnosis [10-12], inverter topology [13, 14], and control strategy [4, 6, 7, 15-21]. In this research, a control strategy is presented, experimental results are given, and first of all, the related studies regarding control strategies for FTC of 3Ph IM drives against SPOF and their contribution will be reviewed.

The control strategies for FTC of 3Ph IM drives under SPOF can be done by the reconfiguration of the remaining healthy stator currents. By rearranging the remaining healthy stator currents, the Magneto-Motive Force (MMF) of the faulty 3Ph IM can be obtained as the MMF of the motor before the fault [15]. Therefore, the faulty 3Ph IM can operate continuously. Based on the above idea, in [16, 17] two scalar control strategies for star-connected and delta-connected 3Ph IM drives under SPOF were presented. The advantages of these techniques are simplicity and suitable for real time implementation. But, they are not appropriate for high performance control of 3Ph IM drives. In order to control 3Ph IM drives with high performances Field-Oriented Control (FOC) or vector control strategies are preferred.

In literature, different FOC strategies for 3Ph IM drives

during SPOF were achieved [4, 7, 15, 18-21]. According to [4], vector control approaches for 3Ph IM drives during SPOF are divided into Indirect FOC (IFOC) and Direct FOC (DFOC). In IFOC methods, the motor flux is calculated based on dynamic model of the motor and in DFOC methods, the motor flux is measured using a sensor or it can be estimated using an observer. IFOC strategies such as [7, 15, 19, 20] due to using a pure integration for calculation of the flux suffer from some problems such as drift, saturation, and etc. To solve pure integration problems, DFOC methods are more preferable than IFOC methods. Paper [18] proposed a DFOC strategy for the faulty 3Ph IM drive based on Extended Kalman Filter (EKF). Nevertheless, this method is complex to implement. Another problem of the used EKF in [18] is the optimization of the covariance matrices. In addition to the above problems, due to using different unbalanced transformation matrices, the used control systems in [7, 18-20] have complex calculations and their implementations are very difficult. In [21], a DFOC technique for the faulty 3Ph IM drive using a flux observer was proposed. The proposed flux observer in [21] uses many pure differential terms. Furthermore, the proposed control system in [21] was only verified by simulations.

In this paper, a simple method for Direct Rotor FOC (DRFOC) of star-connected 3Ph IM drives under SPOF using a flux linkage observer for the rotor flux estimation is proposed. Two advantages can be achieved in the proposed control system. Firstly, the proposed control method has good performances over a wide range of speed including low speed operation. Secondly, the used flux linkage observer has simple structure and with some changes can be utilized during normal and SPOF conditions. A DSP/TMS320F28335 based 1HP star-connected 3Ph IM variable speed system is setup for experiments. Experimental results validate the correctness of the proposed DRFOC algorithm.

This research is divided into six sections. Section 2 shows the used inverter topology. Section 3 presents the dynamic model of the faulty 3Ph IM. The proposed FTC algorithm is discussed in Section 4. This section deals with the FOC equations of the faulty 3Ph IM, the proposed flux linkage observer, and the introduced FTC scheme. The effectiveness of the control method is verified by experiment tests in Section 5. The last section is the conclusion.

2. The used inverter topology

In literature, different inverter topologies for star-connected 3Ph motor drives during SPOF were proposed. Generally, in order to control a star-connected 3Ph motor under SPOF, the Neutral Point of the Motor (NPM) should be accessible. To drive the faulty 3Ph motor, the NPM can be connected to the mid-point of the capacitor bank or it can be connected to the fourth leg of inverter [13, 14]. The used inverter topology in this paper is based on [15] and it is shown in Figure 1. It is worth noting that this topology is a cost-saving solution, no additional hardware power or electronics components are required.
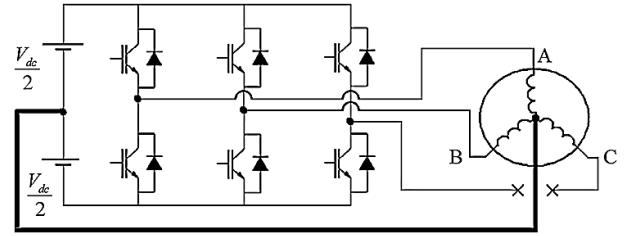
Figure 1. The used inverter topology

According to Figure 1, the maximum motor speed of the 3Ph IM drive during SPOF reduces to half of its nominal value as the applied voltage on the faulty 3Ph IM reduces to half of its original value. Moreover, under the limit of maximum currents in the inverter leg, the maximum torque of the 3Ph IM drive during SPOF reduces to 1/3 of the maximum torque of the healthy 3Ph IM drive [13].

3. Dynamic model of the faulty 3Ph IM

Considering the availability of the NPM, the dynamic model of a star-connected 3Ph IM during SPOF in a stationary frame can be written as (1)-(6) [21]:

$$\begin{bmatrix} v_{ds}^s \\ v_{qs}^s \end{bmatrix} = \begin{bmatrix} r_s + L_{ds}\dfrac{d}{dt} & 0 \\ 0 & r_s + L_{qs}\dfrac{d}{dt} \end{bmatrix} \begin{bmatrix} i_{ds}^s \\ i_{qs}^s \end{bmatrix} + \begin{bmatrix} L_{dm}\dfrac{d}{dt} & 0 \\ 0 & L_{qm}\dfrac{d}{dt} \end{bmatrix} \begin{bmatrix} i_{dr}^s \\ i_{qr}^s \end{bmatrix}$$

(1)

$$\begin{bmatrix} v_{dr}^s \\ v_{qr}^s \end{bmatrix} = \begin{bmatrix} 0 \\ 0 \end{bmatrix} = \begin{bmatrix} L_{dm}\dfrac{d}{dt} & \Omega_r L_{qm} \\ -\Omega_r L_{dm} & L_{qm}\dfrac{d}{dt} \end{bmatrix} \begin{bmatrix} i_{ds}^s \\ i_{qs}^s \end{bmatrix} + \begin{bmatrix} r_r + L_r\dfrac{d}{dt} & \Omega_r L_r \\ -\Omega_r L_r & r_r + L_r\dfrac{d}{dt} \end{bmatrix} \begin{bmatrix} i_{dr}^s \\ i_{qr}^s \end{bmatrix}$$

(2)

$$\begin{bmatrix} \psi_{ds}^s \\ \psi_{qs}^s \end{bmatrix} = \begin{bmatrix} L_{ds} & 0 \\ 0 & L_{qs} \end{bmatrix} \begin{bmatrix} i_{ds}^s \\ i_{qs}^s \end{bmatrix} + \begin{bmatrix} L_{dm} & 0 \\ 0 & L_{qm} \end{bmatrix} \begin{bmatrix} i_{dr}^s \\ i_{qr}^s \end{bmatrix}$$

(3)

$$\begin{bmatrix} \psi_{dr}^s \\ \psi_{qr}^s \end{bmatrix} = \begin{bmatrix} L_{dm} & 0 \\ 0 & L_{qm} \end{bmatrix} \begin{bmatrix} i_{ds}^s \\ i_{qs}^s \end{bmatrix} + \begin{bmatrix} L_r & 0 \\ 0 & L_r \end{bmatrix} \begin{bmatrix} i_{dr}^s \\ i_{qr}^s \end{bmatrix}$$

(4)

$$\tau_e = \frac{P}{2}\left(L_{qm} i_{qs}^s i_{dr}^s - L_{dm} i_{ds}^s i_{qr}^s \right)$$

(5)

$$\tau_e - \tau_l = \frac{2}{P}\left(J\frac{d\Omega_r}{dt} + B\Omega_r \right)$$

(6)

where,

$$L_{ds} = L_{ls} + 1.5L_{ms} \quad , \quad L_{qs} = L_{ls} + 0.5L_{ms}$$
$$L_{dm} = 1.5L_{ms} \quad , \quad L_{qm} = \sqrt{3}/2 L_{ms}$$

(7)

In (1)-(7), rs, rr are the stator and rotor resistances. L_{ds}, L_{qs}, L_r, L_{dm}, L_{qm} denote the stator and rotor self and mutual inductances. v_{ds}^s, v_{qs}^s are the stator (d-q) axes voltages. v_{dr}^s, v_{qr}^s are the rotor (d-q) axes voltages. i_{ds}^s, i_{qs}^s are the stator (d-q) currents. i_{dr}^s, i_{qr}^s are the rotor (d-q) currents. ψ_{ds}^s, ψ_{qs}^s are the stator (d-q) fluxes. ψ_{dr}^s, ψ_{qr}^s are the rotor (d-q) fluxes. τ_e, τ_l are electromagnetic torque and load torque. Ω_r is the motor speed. *P, J, B* are the number of poles, moment of inertia, and viscous friction coefficient, respectively.

It is worth noting that in this paper, superscripts "s" and "e" indicate stationary and rotating reference frames, respectively.

4. Proposed FTC algorithm

In this section, the proposed FTC algorithm for DRFOC of the faulty 3Ph IM is presented. Firstly, FOC equations of the faulty 3Ph IM using a suitable unbalanced transformation matrix is presented. Then, the proposed flux linkage observer for estimation of the rotor flux is discussed. Finally, the introduced FTC scheme is given.

4.1. FOC equations of the faulty 3Ph IM

The stator (d-q) MMF of a 3Ph IM in the rotating reference frame and during normal mode (F_{ds}^{en}, F_{qs}^{en}) are as follows:

$$F_{ds}^{en} = F_{ds}^{sn} \cos\xi_e + F_{qs}^{sn} \sin\xi_e$$

(8)

$$F_{qs}^{en} = -F_{ds}^{sn} \sin\xi_e + F_{qs}^{sn} \cos\xi_e$$

(9)

where, F_{ds}^{sn}, F_{qs}^{sn} are the stator (d-q) MMF of a 3Ph IM in the stationary reference frame and during normal mode. Moreover, ξ_e is the rotor flux angle. The 3Ph IM during SPOF is equivalent to a 2Ph IM with different turn numbers [21]. Consequently, F_{ds}^{sf}, F_{qs}^{sf}(the stator (d-q) MMF of a 3Ph IM in the stationary reference frame and during SPOF) can be written as (10) and (11):

$$F_{ds}^{sf} = T_d i_{ds}^s$$

(10)

$$F_{qs}^{sf} = T_q i_{qs}^s$$

(11)

where, T_d and T_q are the turn numbers of (d-q) axes. According to (8)-(11) and using $F_{ds}^{sn} = F_{ds}^{sf}$ and $F_{qs}^{sn} = F_{qs}^{sf}$ we can write:

$$F_{ds}^{en} = T_d i_{ds}^s \cos\xi_e + T_q i_{qs}^s \sin\xi_e$$

(12)

$$F_{qs}^{en} = -T_d i_{ds}^s \sin\xi_e + T_q i_{qs}^s \cos\xi_e$$

(13)

Based on (12) and (13) and assuming $T_d / T_q = L_{dm} / L_{qm}$ and $\begin{bmatrix} F_{ds}^{en}/T_q & F_{qs}^{en}/T_q \end{bmatrix}^T = \begin{bmatrix} i_{ds}^e & i_{qs}^e \end{bmatrix}^T$, an

unbalanced transformation matrix ($\left[k_s^{ef} \right]$) is achieved as (14):

$$\begin{bmatrix} i_{ds}^e \\ i_{qs}^e \end{bmatrix} = \left[k_s^{ef} \right] \begin{bmatrix} i_{ds}^s \\ i_{qs}^s \end{bmatrix} = \begin{bmatrix} (L_{dm} / L_{qm})\cos\xi_e & \sin\xi_e \\ -(L_{dm} / L_{qm})\sin\xi_e & \cos\xi_e \end{bmatrix} \begin{bmatrix} i_{ds}^s \\ i_{qs}^s \end{bmatrix} \tag{14}$$

Applying (14) and using $\psi_{dr}e=|\psi_r|$ and $\psi_{qr}e=0$, the vector control equations of the 3Ph IM during SPOF can be achieved as (15) and (16):

$$|\psi_r| = L_{qm} i_{ds}^e - \frac{L_r}{r_r}\frac{d|\psi_r|}{dt} \tag{15}$$

$$\tau_e = \frac{P}{2}\frac{L_{qm}}{L_r}|\psi_r| i_{qs}^e \tag{16}$$

4.2.   Proposed flux linkage observer

For vector-controlled 3Ph IM drive systems, the flux amplitude and angle are required. In this section, based on the dynamic model of the faulty 3Ph IM, a rotor flux linkage observer is presented. According to (1)-(4), the faulty 3Ph IM fluxes in terms of stator (d-q) currents, rotor (d-q) fluxes, stator (d-q) fluxes, and stator (d-q) voltages can be written as (17)-(19):

$$\begin{bmatrix} \dfrac{d\psi_{dr}^s}{dt} \\ \dfrac{d\psi_{qr}^s}{dt} \end{bmatrix} = \begin{bmatrix} \dfrac{r_r L_{dm}}{L_r} i_{ds}^s \\ \dfrac{r_r L_{qm}}{L_r} i_{qs}^s \end{bmatrix} - \begin{bmatrix} \dfrac{r_r}{L_r} & \Omega_r \\ -\Omega_r & \dfrac{r_r}{L_r} \end{bmatrix} \begin{bmatrix} \psi_{dr}^s \\ \psi_{qr}^s \end{bmatrix} \tag{17}$$

$$\begin{bmatrix} \psi_{dr}^s \\ \psi_{qr}^s \end{bmatrix} = \begin{bmatrix} L_{dm} - \dfrac{L_r L_{ds}}{L_{dm}} & 0 \\ 0 & L_{qm} - \dfrac{L_r L_{qs}}{L_{qm}} \end{bmatrix} \begin{bmatrix} i_{ds}^s \\ i_{qs}^s \end{bmatrix} + \begin{bmatrix} \dfrac{L_r}{L_{dm}} & 0 \\ 0 & \dfrac{L_r}{L_{qm}} \end{bmatrix} \begin{bmatrix} \psi_{ds}^s \\ \psi_{qs}^s \end{bmatrix} \tag{18}$$

$$\begin{bmatrix} \dfrac{d\psi_{ds}^s}{dt} \\ \dfrac{d\psi_{qs}^s}{dt} \end{bmatrix} = \begin{bmatrix} v_{ds}^s \\ v_{qs}^s \end{bmatrix} - \begin{bmatrix} r_s & 0 \\ 0 & r_s \end{bmatrix} \begin{bmatrix} i_{ds}^s \\ i_{qs}^s \end{bmatrix} \tag{19}$$

According to (17)-(19), the flux linkage observer can be exposed as Figure 2.

Figure 2. Flux linkage observer

As shown in Figure 2, the stator (d-q) fluxes according to (19) are calculated and they are used in (18) for calculation of the rotor (d-q) fluxes. Equations (17) and (18) calculate the rotor (d-q) fluxes. The error between two rotor flux calculators after passing from a PI controller produces a voltage error signal and can be utilized in (19). Finally, the rotor flux amplitude and angle can be determined as shown in Figure 2.

4.3.   Introduced FTC scheme

Based on (15), (16), and Figure 2, the proposed FTC scheme for DRFOC of star-connected 3Ph IM drives under SPOF can be shown as Figure 3.

Figure 3. The proposed FTC scheme for DRFOC of star-connected 3Ph IM drives under SPOF

In Figure 3 [21]:

$$[k_s] = \frac{\sqrt{2}}{2}\begin{bmatrix} 1 & -1 \\ 1 & 1 \end{bmatrix} \tag{20}$$

It is worth noting that Figure 3 can be used for a healthy star-connected 3Ph IM drive using the following parameters and transformation matrix [22]:

$$L_{ds} = L_{qs} = L_{ls} + 1.5L_{ms} \quad , \quad L_{dm} = L_{qm} = 1.5L_{ms}$$

$$(21)$$

$$[k_s] = \sqrt{2/3} \begin{bmatrix} 1 & -0.5 & -0.5 \\ 0 & \sqrt{3}/2 & -\sqrt{3}/2 \end{bmatrix}$$

$$(22)$$

Moreover, Figure 3 can be used for a faulty star-connected 3Ph IM drive using the parameters as shown in (7).

The proposed control technique of Figure 3 which is based on an unbalanced transformation matrix for the stator current components introduces an efficient method to control the faulty drive system, avoiding the complexity of calculating of the backward voltages.

5. Experiment tests

In order to check the theoretical study shown in the previous sections some experiments have been performed. In tests, fast fault detection based on Ref. [18] is considered. The photograph of the test bench is illustrated in Figure 4. The used test bench for assessment of the performance of the proposed drive system consists of three main sections:

• A 1HP star-connected 3Ph IM which is coupled to a DC generator and it is supplied by a three-leg voltage source inverter

• Three Hall-effect current sensors and an incremental encoder

• The control strategy is implemented using PSIM and

DSP/TMS320F28335
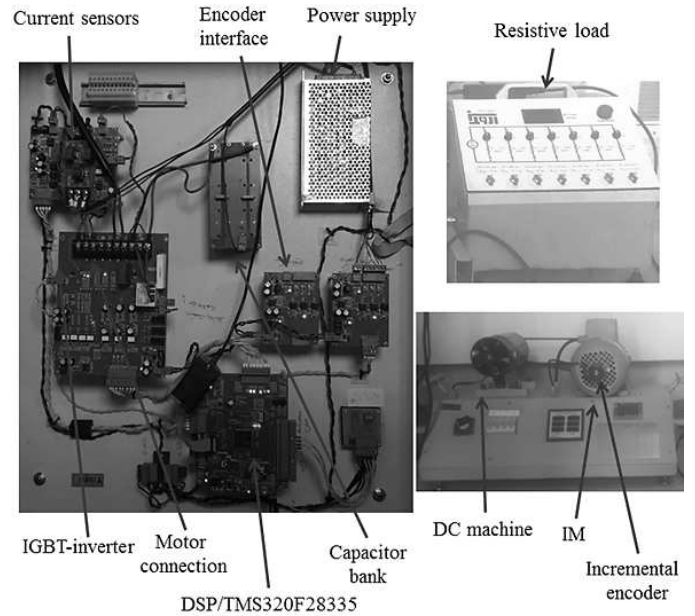
Figure 4. The photograph of the test bench

The parameters of the 3Ph IM are listed in Table 1.

Table 1. The parameters of the 3Ph IM

F	r_s	r_r	L_{dm}	$L_{ls}=L_{lr}$	J	P
50Hz	10.44Ω	14.64Ω	0.597H	0.0167H	0.016kg.m²	2

This part shows the different experimental results obtained with the introduced FTC system in this research, the presented FTC system based on Ref. [7], and the classical IRFOC strategy based on Ref. [22]. The experimental tests have been performed under different operating conditions: normal state and SPOF.

An experimental result for FTC of the 3Ph IM is shown in Figure 5. As shown in this figure, the 3Ph IM speed changes from 50rad/s to 120rad/s and from 120rad/s to 50rad/s. Furthermore, in this figure, τl=1N.m (50% of the permissible load). In addition, $|\psi_r|^* = 1wb$. Figure 5 shows the experimental results of the rotation speed, stator phase currents, torque, rotor flux amplitude, and rotor flux angle during healthy and SPOF modes. In this test, at first the 3Ph IM operates without abnormalities in the operation of the drive. Then, a SPOF happens in phase "c".
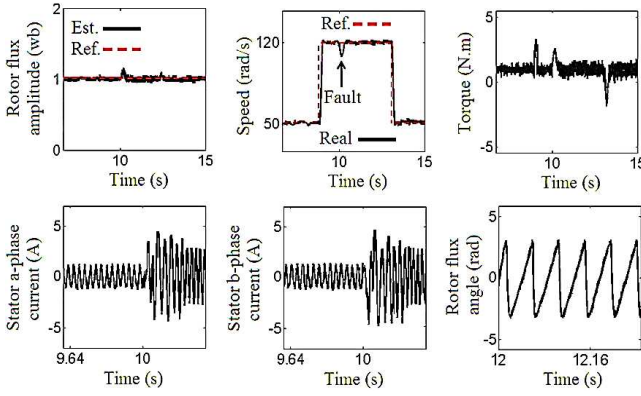
Figure 5. Experimental result for FTC of the 3Ph IM

The results of Figure 5 show that the steady-state speed, rotor flux amplitude, and torque responses of the faulty drive are close enough to the healthy drive system with slightly higher ripples. In addition, the results demonstrate that the transient time for speed, rotor flux, and torque responses of the healthy and faulty drives are almost the same. The healthy and faulty 3Ph IM phase currents are sinusoidal. Moreover, the steady-state peak phase currents of the faulty drives are bigger than healthy drive as expected. This figure shows the good performance of the proposed FTC approach under load condition and speed changes.

In the second scenario, for the faulty 3Ph IM different experiments have been carried out to evaluate the performance of the proposed controller at low speed operation. The experimental results for the proposed controller in this paper, the presented method in Ref. [7], and the classical IRFOC strategy based on Ref. [22] are shown in Figure 6(a)-Figure 6(c), respectively. It is worth noting that, in the experimental results of Figure 6(a)-Figure 6(c) the NPM is connected to the mid-point of the capacitor bank. As exposed in this figure, the 3Ph IM speed is 1rad/s. Additionally, $\left|\psi_r\right|^* = 1\text{wb}$. Figure 6 shows the experimental results of the rotation speed, torque, and rotor flux amplitude for the faulty 3Ph IM.

(a)   (b)   (c)
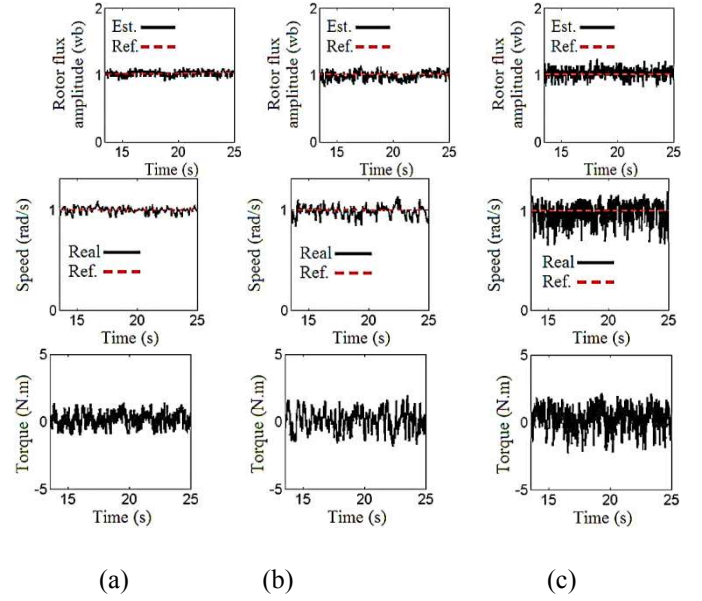
Figure 6. Experimental result of different control methods for the faulty 3Ph IM at low speed operation; (a) proposed controller in this paper, (b) presented method in Ref. [7], (c) classical IRFOC strategy based on Ref. [22]

As expected, using the classical IRFOC strategy severe speed, flux, and torque oscillations appears (see Figure 6(c)). In addition, the results confirm the efficiency of the proposed real-time FTC system for SPOF in the 3Ph IM drive at low speed operation (see Figure 6(a)). The comparison between Figure 6(a) and Figure 6(b) show that after the presence of SPOF, the ripples of the speed, flux, and torque of the presented method in Ref. [7] are bigger than that of the proposed FTC strategy in this paper.

6. Conclusion

This research proposes a simple approach for FTC of SPOF in star-connected 3Ph IM drives. The proposed approach is based on a modified RFOC technique in cooperation with a flux linkage observer. The FTC approach by only some modifications in the 3Ph IM parameters and the transformation matrix can be shared during normal and SPOF modes. The experimental results show that the proposed FTC strategy permits the continuous operation of the 3Ph IM drive during low and high speeds even under a load condition. The proposed FTC method of the 3Ph IM has good fault tolerant capability and tracking performance and is appropriate for high performance and high reliability driving cases. The proposed method can also be extended to FTC of multiphase IMs in the case of SPOF.

References

[1] H. Ismail, et al., "Constant Switching Frequency and Torque Ripple Minimization of DTC of Induction Motor Drives with Three-level NPC Inverter," International Journal of Power Electronics and Drive Systems, vol. 8, pp. 1035, Sep 2017.

[2] Y. Yu, et al., Current sensor fault diagnosis and tolerant control for VSI-based induction motor drives," IEEE Transactions on Power Electronics, vol. 33, pp. 4238-4248, Jun 2017.

[3] A. Jidin, et al., "Improvement of Torque Capability of Direct Torque Control of Induction Machines," International Journal of Power Electronics and Drive Systems, vol. 8, Sep 2017.

[4] R. Tabasian, et al., "Control of Three-Phase Induction Machine Drives During Open-Circuit Fault: A Review," IETE Journal of Research, pp. 1-18, Feb 2020.

[5] M. Manohar and S. Das, "Current sensor fault-tolerant control for direct torque control of induction motor drive using flux-linkage observer," IEEE Transactions on Industrial Informatics, vol. 13, pp. 2824-2833. Jun 2017.

[6] M. Tousizadeh, et al., "Fault-tolerant field-oriented control of three-phase induction motor based on unified feedforward method," IEEE Transactions on Power Electronics, vol. 34, pp. 7172-7183, Dec 2018.

[7] M. Jannati, et al., "Performance Evaluation of the Field-Oriented Control of Star-Connected 3-Phase Induction Motor Drives under Stator Winding Open-Circuit Faults," Journal of Power Electronics, vol. 16, pp. 982-993, May 2016.

[8] W. Wang, et al., "Common model predictive control for permanent-magnet synchronous machine drives considering single-phase open-circuit fault," IEEE Transactions on Power Electronics, vol. 32, pp. 5862-5872, Oct 2016.

[9] B. Tian, et al., "Cancellation of torque ripples with FOC strategy under two-phase failures of the five-phase PM motor," IEEE Transactions on Power Electronics, vol. 32, pp. 5459-5472, Aug 2016.

[10] A. Hajary, et al., "Detection and Localization of Open-Phase Fault in Three-Phase Induction Motor Drives Using Second Order Rotational Park Transformation," IEEE Transactions on Power Electronics, vol. 34, pp. 11241-11252, Feb 2019.

[11] J. O. Estima and A. J. M. Cardoso, "A new approach for real-time multiple open-circuit fault diagnosis in voltage-source inverters," IEEE transactions on industry applications, vol. 47, pp. 2487-2494, Sep 2011.

[12] H. Yan, et al., "A novel open-circuit fault diagnosis method for voltage source inverters with a single current sensor," IEEE Transactions on Power Electronics, vol. 33, pp. 8775-8786, Nov 2017.

[13] M. Tousizadeh, et al., "Performance comparison of fault-tolerant three-phase induction motor drives considering current and voltage limits," IEEE Transactions on Industrial Electronics, vol. 66, pp. 2639-2648, Jul 2018.

[14] B. A. Welchko, et al., "Fault tolerant three-phase AC motor drive topologies: a comparison of features, cost, and limitations," IEEE Transactions on power electronics, vol. 19, pp. 1108-1116, Jul 2004.

[15] T. H. Liu, et al., "A strategy for improving reliability of field-oriented controlled induction motor drives," IEEE transactions on industry applications, vol. 29, pp. 910-918, Sep 1993.

[16] D. Kastha and B. K. Bose, "Fault mode single-phase operation of a variable frequency induction motor drive and improvement of pulsating torque characteristics," IEEE Transactions on Industrial Electronics, vol. 41, pp. 426-433, Aug 1994.

[17] A. Sayed-Ahmed and N. A. Demerdash, "Control of Open-Loop PWM Delta-Connected Motor-Drive Systems under One Phase Failure Condition," Journal of Power Electronics, vol. 11, pp. 824-836, 2011.

[18] M. Nikpayam, et al., "Fault-tolerant control of Y-connected three-phase induction motor drives without speed measurement," Measurement, vol. 149, pp. 106993, Jan 2020.

[19] M. Jannati, et al., "Modeling and RFOC of faulty three-phase IM using Extended Kalman Filter for rotor speed estimation," In 8th International Power Engineering and Optimization Conference (PEOCO2014), pp. 270-275, Mar 2014.

[20] M. Jannati, et al., "A novel method for IRFOC of three-phase induction motor under open phase fault," International Journal of Power Electronics and Drive System (IJPEDS), vol. 6, pp. 439-448, Sep 2013.

[21] Y. Zhao and T. A. Lipo, "An approach to modeling and field-oriented control of a three phase induction machine with structural imbalance," In Proceedings of Applied Power Electronics Conference (APEC'96), Mar 1996.

[22] P. Vas, "Sensorless vector and direct torque control," Oxford Univ. Press, 1998.